

Title	Chain packing and its anomalous effect on mechanical toughness for poly(lactic acid)
Author(s)	Huang, Tong; Miura, Motohiro; Nobukawa, Shogo; Yamaguchi, Masayuki
Citation	Biomacromolecules, 16(5): 1660-1666
Issue Date	2015-04-15
Type	Journal Article
Text version	author
URL	<a href="http://hdl.handle.net/10119/12867">http://hdl.handle.net/10119/12867</a>
Rights	Tong Huang, Motohiro Miura, Shogo Nobukawa, and Masayuki Yamaguchi, Biomacromolecules, 2015, 16(5), pp.1660-1666. This document is the unedited author's version of a Submitted Work that was subsequently accepted for publication in Biomacromolecules, copyright (c) American Chemical Society after peer review. To access the final edited and published work, see <a href="http://dx.doi.org/10.1021/acs.biomac.5b00293">http://dx.doi.org/10.1021/acs.biomac.5b00293</a>
Description	

# **Chain packing and its anomalous effect on mechanical toughness for poly(lactic acid)**

*Tong Huang, Motohiro Miura, Shogo Nobukawa,  
Masayuki Yamaguchi\**

School of Materials Science,  
Japan Advanced Institute of Science and Technology  
1-1 Asahidai, Nomi, Ishikawa 923-1292 JAPAN

---

\* To whom correspondence should be addressed:  
Phone +81-761-51-1621, Fax +81-761-51-1625  
E-mail: m\_yama@jaist.ac.jp

**Abstract**

In this study, the effect of chain packing on tensile properties is studied employing amorphous poly(lactic acid) PLA. It is found that the samples cooled in the temperature range from 60 to 80 °C, i.e., slightly higher than the glass transition temperature  $T_g$ , show ductile behavior with a low brittle-ductile transition temperature. Furthermore, the sample obtained by prolonged cooling at 56 °C also shows ductile behavior, whereas a shorter cooling time at the same temperature leads to brittle fracture. Even for the samples quenched at 40 °C, the exposure to post-processing annealing operation at 60 °C enhances the toughness greatly, which is an anomalous phenomenon for a glassy polymer. The dynamic mechanical analysis and thermal characterization reveal that the ductile samples show slightly higher  $T_g$  than the brittle samples, presumably due to the high packing density of polymer chains. Moreover, it is found from infrared spectroscopy that the ductile samples show strong absorbance at 1267  $\text{cm}^{-1}$ , ascribed to high-energy *gg* conformers. Following the classic Robertson's descriptions of plastic flow, it is concluded that the increase in the *gg* conformers, which show the conformation change under a low stress level, reduces the critical onset stress for shear yielding. The results demonstrate that the mechanical toughness of PLA can be controlled by the cooling conditions during processing and the post-processing annealing operation.

**Keywords:** Poly(lactic acid); Toughness; Mechanical properties; Processing

## Introduction

In recent years, polymeric materials produced from biomass have been researched intensively because of concerns about the global environment and the decrease in petroleum resources. Poly(lactic acid) (PLA), a biomass-derived plastic, exhibits several attractive properties such as biodegradability, high modulus, high strength and excellent clarity. Therefore, it is a promising polymeric material with the potential to replace petroleum-based polymers. However, the drawbacks of PLA, such as its slow crystallization rate and mechanical brittleness, limit its usefulness in practical applications.<sup>1-5</sup> In particular, the poor mechanical properties have to be improved greatly because the strain at break is lower than 10 %.<sup>6</sup> Since its tensile strength and elastic modulus are comparable to those of conventional petroleum-based plastics such as polypropylene and polystyrene, the improvement of its mechanical toughness will widen the potential range of applications.<sup>7</sup>

Several approaches have been explored in order to improve the mechanical toughness of PLA. The incorporation of a rubbery phase into a PLA matrix has been recognized as an efficient method. Kowalczyk and Piorkowska reported that the ductility and toughness of PLA were apparently enhanced with a small amount of natural rubber (NR).<sup>8</sup> Recently, Zhang et al. reported that the strain at break and impact strength are enhanced by the addition of expoxidized natural rubber.<sup>9</sup> Zhao et al. found a significant improvement in tensile toughness was achieved by mixing of ultrafine full-vulcanized rubber particles.<sup>10</sup>

Meanwhile, basic researches on polymer fracture have been carried out

intensively.<sup>11-19</sup> It is generally understood that there are two main mechanisms for the plastic fracture of a polymer solid; one is crazing and the other is shear yielding. Crazing, which often results in brittle fractures, takes place with void-opening, whereas shear yielding, which occurs with the conformation change of polymer chains, leads to ductile deformation. Since the critical onset stress of shear yielding is more sensitive to the strain rate and ambient temperature as compared with that of crazing, ductile deformation occurs at high temperature or low strain rate.<sup>20,21</sup> Moreover, processing conditions, such as the annealing operation, have been known to affect the deformation behavior. Melick et al. found that the annealed polycarbonate (PC) shows brittle fracture because of the increase in onset stress of shear yielding.<sup>22</sup> Recently, Cheng et al. have also reported the brittle fracture for PC annealed at 135 °C for one month.<sup>23</sup> They concluded that the annealing operation enhances the inter-segmental interactions and thus increases the yield stress, leading to brittle fracture. Pan et al. studied the effect of aging time on the mechanical properties of poly(L-lactic acid) (PLLA) annealed at temperature below  $T_g$ . They found that the strain at break of PLLA is significantly decreased by the exposure to the annealing operation. Moreover, they pointed out that the high level of packing density of polymer chains leads to brittle fracture is common with other plastics.<sup>24</sup> However, to the best of our knowledge, there have been no reports on the improved mechanical toughness of pure PLA obtained by increasing the chain packing, which can be provided by adjusting the processing conditions such as cooling temperature and post-processing annealing operation.

In this paper, the effect of processing condition during compression-molding on

the tensile properties of PLA was investigated considering the chain packing. It should be noted that the appropriate cooling condition enhances the toughness of pure PLA. A review of the relevant literatures<sup>1-7,11-15</sup> indicates that such phenomena have not been reported before. Moreover, the brittle-ductile transition temperature for PLA was also investigated.

## **Experimental Section**

### **Materials**

The polymeric material employed in this study was a commercially available poly(lactic acid) (PLA) (Lacea H280, Mitsui Chemicals). The content of D-lactic unit is 12%. Due to the high content of D-lactic unit, it does not show crystallinity. The number- and weight-average molecular weights, evaluated by a gel permeation chromatography (Tosoh, HLC- 8020) with TSK-GEL GMHXL, were  $1.5 \times 10^5$  and  $2.7 \times 10^5$ , respectively, as a polystyrene standard.

After being dried in a vacuum oven at 80 °C for 4 hours, the pellets were compressed into a flat film by a compression-molding machine (Tester Sangyo, Table-type-test press SA-303-I-S) at 200 °C. The samples were then cooled at various cooling conditions by the cooling unit (TGK, FCW-10). Finally, all samples were cooled again in an ice water bath for 3 min and maintained at -20 °C in a freezer in order to prevent aging process prior to the measurements. The film thickness was adjusted to be 0.39 - 0.40 mm. Moreover, some samples were exposures to the post-processing annealing operation at 60 °C for 10 min.

In this paper the numerals in the sample code represent the cooling temperature and time. For example, PLA-40-10 denotes sample cooled at 40 °C for 10 min.

## **Measurements**

### ***Tensile properties***

Tensile properties were examined using a uniaxial tensile machine (Tokyo Testing Machine, LSC-50/300) at various temperatures from 5 to 40 °C. Dumbbell-shaped specimens (ASTMD-1822-L) were cut from the film by a dumbbell cutter (Dumbbell, SDL-200). The initial gage length was 10 mm. One of the cross-heads moved at a constant speed of 10 mm/min. Therefore, the initial strain rate was 0.017 s<sup>-1</sup>. The measurements were performed ten times for each sample and the averaged value was calculated. During the deformation, the sample shape was monitored by a video camera. Furthermore, some samples were taken out from the tensile machine before the rupture to observe the surface morphology by a scanning electron microscope SEM (Hitachi, S4100) and the molecular orientation in the necked region by a polarized optical microscope (Leica, DMLP) with crossed polars.

### ***Dynamical mechanical properties***

Temperature dependence of tensile storage modulus  $E'$  and loss modulus  $E''$  was measured using a rectangular specimen with 5 mm in width, 25 mm in length and 0.4 mm in thickness by a dynamic mechanical analyzer (UBM, Rheogel E4000-DVE) in the temperature range between 25 and 100 °C. The heating rate was 1 °C/min, and the applied frequency was 100 Hz.

### ***Thermal properties***

Thermal analysis was conducted by a differential scanning calorimeter DSC (Perkin Elmer, DSC8500) under a nitrogen atmosphere. The samples were heated from room temperature to 200 °C at a heating rate of 10 °C/min. The weight of the samples in an aluminum pan was approximately 10 mg.

### ***FTIR spectroscopy***

Infrared spectra of the samples cooled at various temperatures were measured using a Fourier-Transform infrared analyzer (Perkin Elmer, Spectrum 100). All spectra were collected with 16 scans and a resolution of 4 cm<sup>-1</sup>. The sample films were prepared by using the same method but with different thicknesses, i.e., approximately 20 μm.

## **Results and Discussion**

Figure 1 shows the stress-strain curves at room temperature for the samples cooled at various temperatures for 10 min at the compression-molding. Both stress and strain are nominal values. It is found that the samples cooled at 0, 40, and 100 °C show brittle fracture around the yield point, which is a well-known behavior for PLA. In contrast, the ductile behavior is observed for the samples cooled at 60 and 80 °C. The strain at break for the ductile samples is larger than 300 %. The results demonstrate that the mechanical toughness of PLA is enhanced by adjusting the cooling temperature, i.e., slightly higher than  $T_g$ .



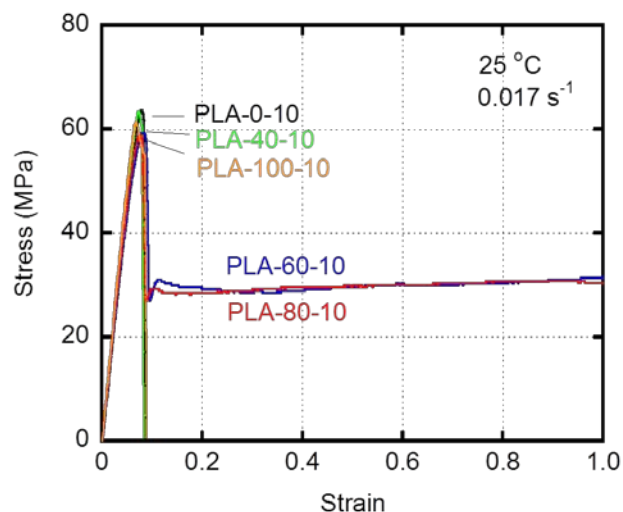


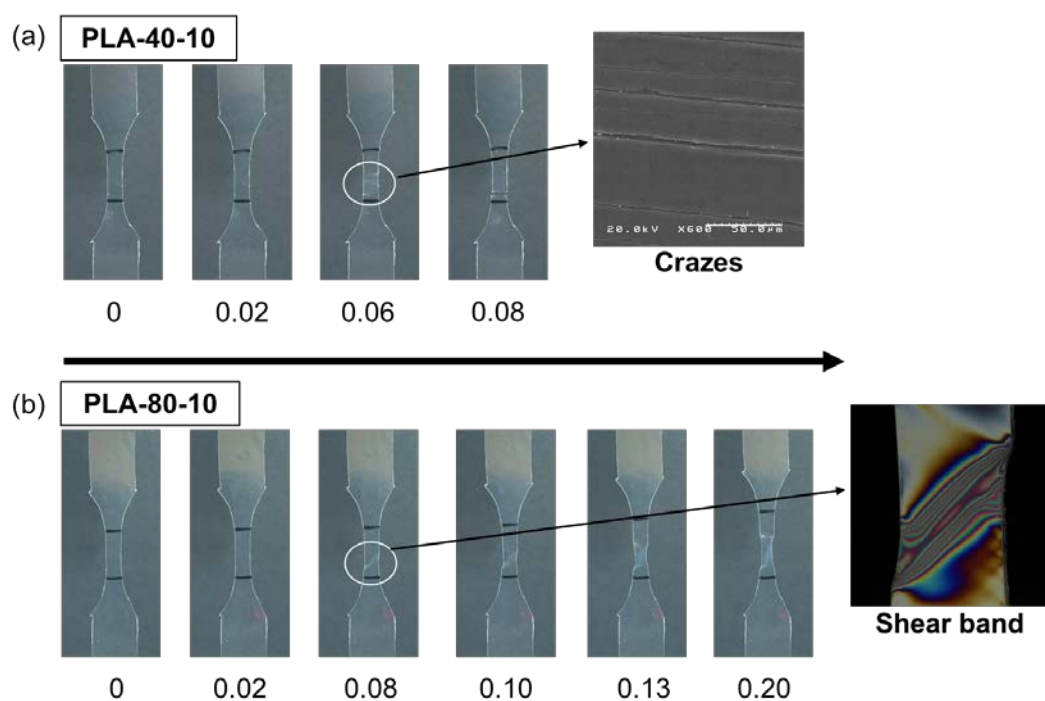
**Figure 1.** Stress-strain curves at room temperature for the samples cooled at various temperatures for 10 min.

The mechanical properties of the samples cooled at various temperatures are summarized in Table 1. It should be noted that the yield stresses of the ductile samples are lower than those of the brittle ones.

**Table 1.** Tensile properties of the samples cooled at various temperatures

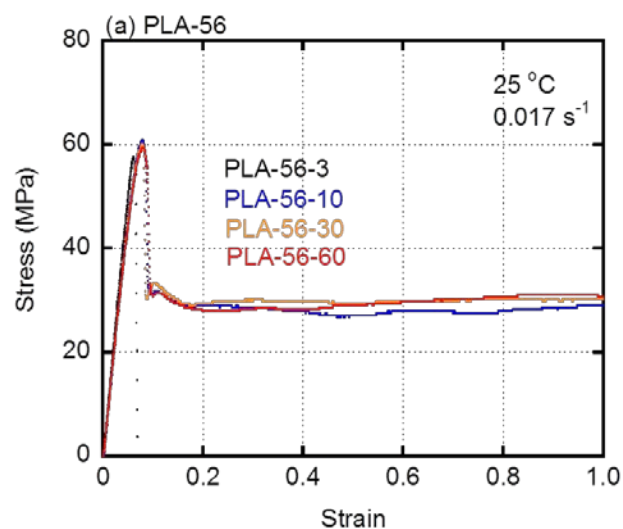
Samples	Strain at break	Tensile Yield Stress (MPa)	Young's Modulus (MPa)
PLA-0-10	$0.079 \pm 0.002$	$63.6 \pm 1.3$	805
PLA-40-10	$0.077 \pm 0.001$	$61.1 \pm 1.6$	794
PLA-60-10	> 3	$60.2 \pm 2.2$	792
PLA-80-10	> 3	$58.1 \pm 1.4$	796
PLA-100-10	$0.078 \pm 0.004$	$61.4 \pm 1.7$	787
PLA-40-10	$0.075 \pm 0.003$	$59.8 \pm 1.0$	797
PLA-40-30	$0.15 \pm 0.08$	$60.3 \pm 1.7$	793
PLA-40-60	$0.13 \pm 0.06$	$61.0 \pm 1.5$	792
PLA-56-3	$0.076 \pm 0.002$	$59.6 \pm 2.0$	810
PLA-56-10	$2.2 \pm 0.7$	$60.9 \pm 1.7$	790
PLA-56-30	$2.9 \pm 0.9$	$60.1 \pm 1.1$	781
PLA-56-60	> 3	$59.3 \pm 1.3$	770

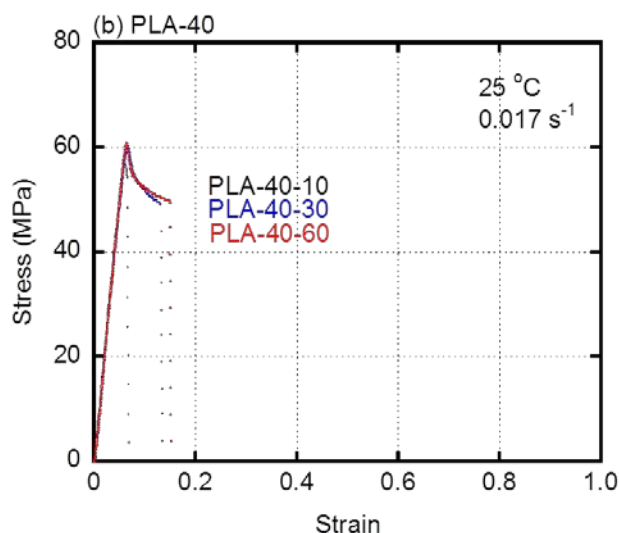
Figure 2 shows the optical photographs of the samples during tensile testing. In the case of PLA-40-10, i.e., a brittle sample, several cracks clearly are detected on the film surface immediately after stretching, as shown in the right-top picture. The cracks develop promptly and result in the brittle failure. This is a typical phenomenon for a brittle polymer.<sup>13,17</sup> In contrast, a shear band appears for the ductile PLA-80-10, instead of the surface cracks, as detected by the polarized optical microscope (right-bottom). The shear band grows to the necking band.



**Figure 2.** Photographs of the samples during the tensile testing at room temperature; (a) cooled at 40 °C for 10 min and (b) cooled at 80 °C for 10 min. The numerals in the figure represent the strain. The SEM picture of the craze is shown in the right-top. The polarized optical microscopy picture of the shear band is shown in the right-bottom.

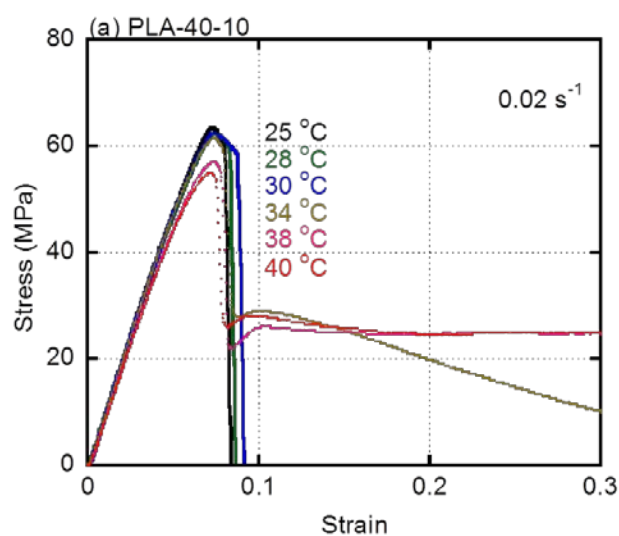
Moreover, it is found that the tensile properties are affected by the cooling time during the compression-molding. Figure 3 shows the stress-strain curves for the samples cooled at 56 °C (PLA-56- $x$ ) and 40 °C (PLA-40- $x$ ) for various cooling times ( $x$  min). As shown in Figure 3(a), the ductile behavior is detected for the samples cooled more than 10 min at 56 °C, whereas PLA-56-3 shows brittle fracture. On the contrary, all samples cooled at 40 °C show brittle behavior, although the strain at break slightly increases with the cooling time. These results indicate that the prolonged cooling slightly lower than  $T_g$  provides the toughness for PLA. Considering the molecular motion, a sample cooled for an extended time at 40 °C will exhibit the ductile behavior. Furthermore, similar to the results shown in Figure 1, the ductile samples show low yield stress as compared with the ultimate stress of the brittle ones. The nonlinear behavior, i.e., the downward deviation from the linear relation of the stress and strain, is detected earlier for the ductile samples, which results in the low yield stress.

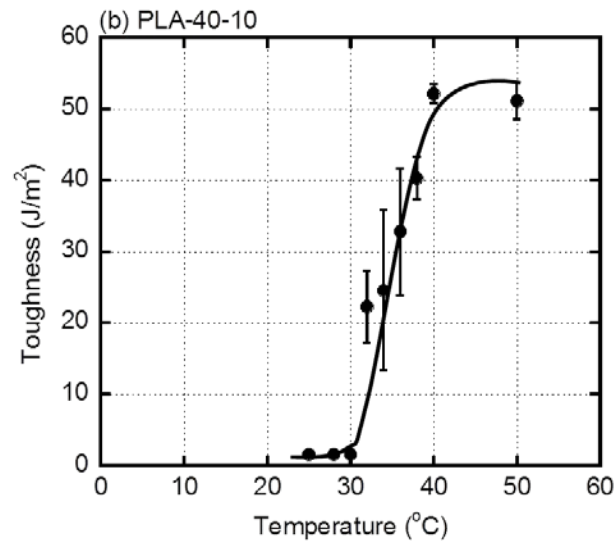




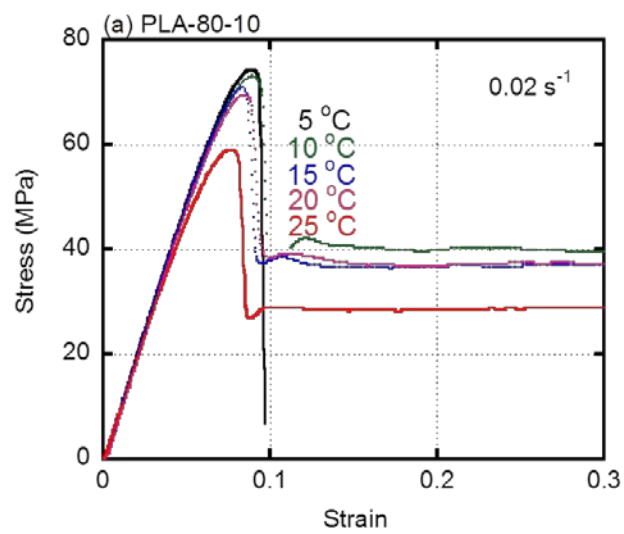
**Figure 3.** Stress-strain curves for the samples cooled at (a) 56 °C and (b) 40 °C for various cooling times.

The tensile testing was performed at various ambient temperatures using PLA-40-10 and PLA-80-10. The area of the stress-strain curve until the rupture is represented as the toughness. As shown in Figure 4 and Figure 5, the brittle-ductile transition is clearly detected for both samples. The transition temperature for PLA-40-10 is found to be around 35 °C, whereas it is 5 °C for PLA-80-10. Thus, PLA-80-10 shows ductile behavior at room temperature.





**Figure 4.** (a) Stress-strain curves for PLA-40-10 at various ambient temperatures and (b) Relation between the ambient temperature and toughness for PLA-40-10.



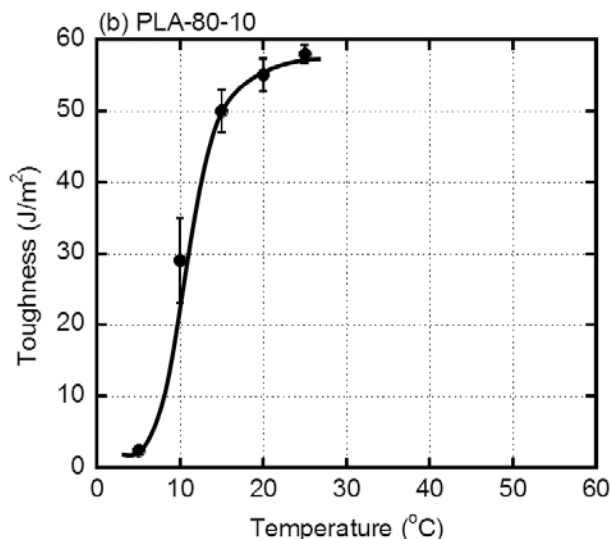


**Figure 5.** (a) Stress-strain curves for PLA-80-10 at various ambient temperatures and (b) Relation between the ambient temperature and toughness for PLA-80-10.

It is confirmed from DSC and wide-angle X-ray diffraction measurements that all samples show no crystallinity. Therefore, the specific volume, which increases with the cooling rate from rubbery or terminal region to glassy one,<sup>25,26</sup> affects the fracture behavior. In other words, the samples with high density chain packing, which is obtained by cooling near  $T_g$ , exhibit ductile behavior. However, the difference in the density is not detected directly by the density measurement because it is significantly small.

There is a slight difference in the dynamic mechanical properties from the brittle and ductile samples. Figure 6 shows the temperature dependence of loss tangent  $\tan \delta$  for the samples cooled at various temperatures for 10 min. The peak is ascribed to  $T_g$  of PLA. The figure demonstrates that the peak shifts slightly toward high temperature with the cooling temperature approaching 80 °C. This slight increase in  $T_g$

is attributed to the closed packing of PLA chains. In the case of PLA-100-10, the first step of cooling was performed at 100 °C, which is higher than  $T_g$ . Then, the sample was quenched to 0 °C on the second step. As a result, the free volume fraction was predictably larger than those cooled at 60 and 80 °C.

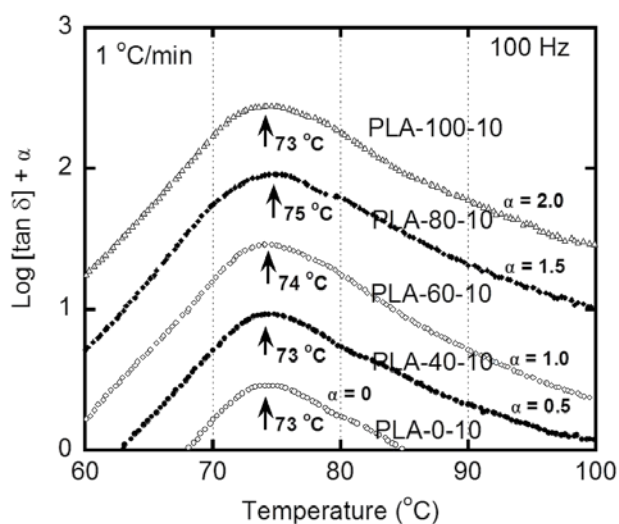


**Figure 6.** Temperature dependence of loss tangent  $\tan \delta$  at 100 Hz for the samples cooled at various temperatures for 10 min. The values are vertically shifted, which are expressed by  $\alpha$ . The arrows represents the peak temperatures. (open circles) PLA-0-10 and  $\alpha = 0$ , (closed circles) PLA-40-10 and  $\alpha = 0.5$ , (open diamonds) PLA-60-10 and  $\alpha = 1.0$ , (closed diamonds) PLA-80-10 and  $\alpha = 1.5$ , and (open triangle) PLA-100-10 and  $\alpha = 2.0$ .

Figure 7 shows the dynamic mechanical spectra for the samples cooled at 56 °C for various times. It is also found that the peak of  $\tan \delta$  shifts slightly toward high temperature as the cooling time increased. This is expectable because the prolonged cooling allows the molecules to be in the equilibrium state.

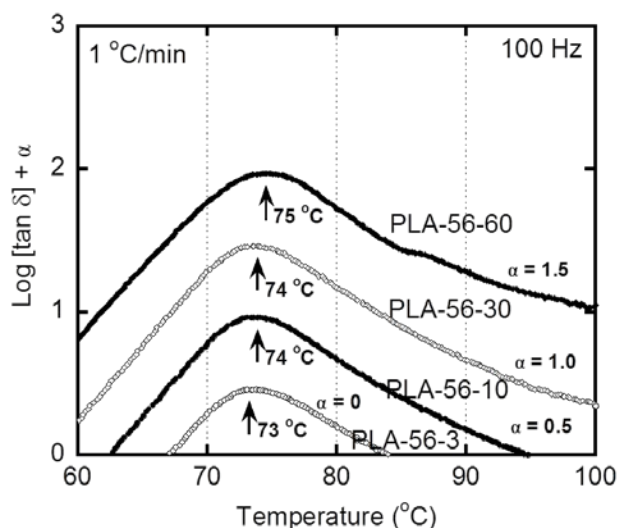


**Figure 7.** Temperature dependence of loss tangent  $\tan \delta$  at 100 Hz for the samples cooled at 56 °C for various cooling times. (open circles) PLA-56-3 and  $\alpha = 0$ , (closed circles) PLA-56-10 and  $\alpha = 0.5$ , (open diamonds) PLA-56-30 and  $\alpha = 1.0$ , and (closed circles) PLA-56-60 and  $\alpha = 1.5$ .

In order to confirm the increase in  $T_g$ , thermal properties are also checked by DSC measurements. The DSC heating curves for the samples cooled at various temperatures are shown in Figure 8. A slight change in  $T_g$  is also detected for the samples, as shown in Table 2, corresponding to the dynamical mechanical spectra.



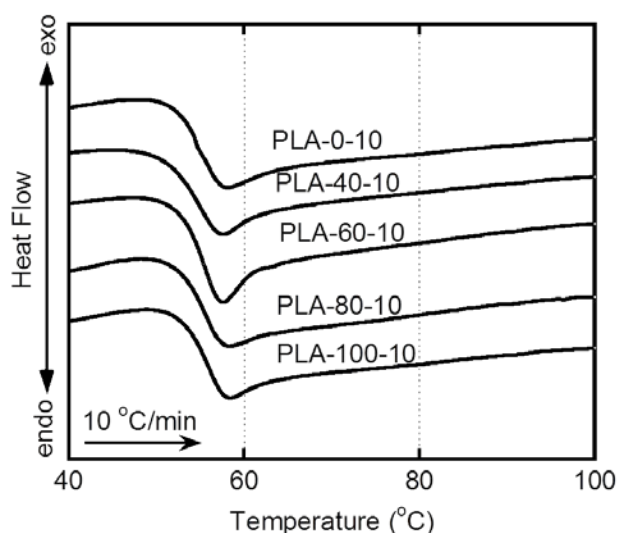


**Figure 8.** DSC heating curves for the samples cooled at various temperatures for 10 min.

**Table 2.** Glass transition temperature  $T_g$  of samples cooled at various temperatures

Samples	$T_g^a$ (°C)	$T_g^b$ (°C)
PLA-0-10	73	53
PLA-40-10	73	53
PLA-60-10	74	54
PLA-80-10	75	55
PLA-100-10	73	53

<sup>a</sup>  $T_g$  is determined by DMA.

<sup>b</sup>  $T_g$  is determined by DSC.

These results suggest that the ductile behavior for the samples with prolonged cooling is attributed to the same reason, i.e., closed packing of amorphous chains. In general, the post-processing annealing operation is well known to increase the shear yielding stress more than crazing stress.<sup>27</sup> Thus, the deformation mechanism changes from ductile to brittle fracture by the exposure to annealing. However, in this study, PLA instead shows ductile deformation without crazing after the annealing operation,

suggesting that high packing density of polymer chains does not increase the onset stress for shear yielding.

According to the physical description of shear yielding given by Robertson et al., a high population of high energy conformers is responsible for the conformation change even under a low stress level, leading to a stable plastic flow of a polymer solid below  $T_g$ .<sup>28-30</sup> Pan et al. studied the conformation change for PLLA during the heating process using an FTIR analyzer.<sup>31</sup> They confirmed that the intensity of the absorbance peak at  $1267\text{ cm}^{-1}$  increases with the ambient temperature. Moreover, they reported that the absorbance peak is highly sensitive to high-energy *gg* conformers in PLA chains. According to them, the rearrangement of PLA chains from the low-energy *gt* conformers to high-energy *gg* conformers occurs near  $T_g$ . In order to investigate the conformation difference of the present samples, FTIR measurements were carried out. Figure 9 shows the FTIR spectra for the samples cooled at various temperatures in the region from  $1240 - 1300\text{ cm}^{-1}$ . The absorbance peak at  $1267\text{ cm}^{-1}$  is ascribed to C-O-C backbone stretching.<sup>32</sup> As seen in the figure, the intensity of  $1267\text{ cm}^{-1}$  band increases with the cooling temperature until  $80\text{ }^\circ\text{C}$ , suggesting that the population of *gg* conformers increases. From the FTIR results, it is reasonable to conclude that the samples cooled at slightly higher than  $T_g$  have the high population of high-energy conformers, leading to a low onset stress for shear yielding by the conformation change during stretching.

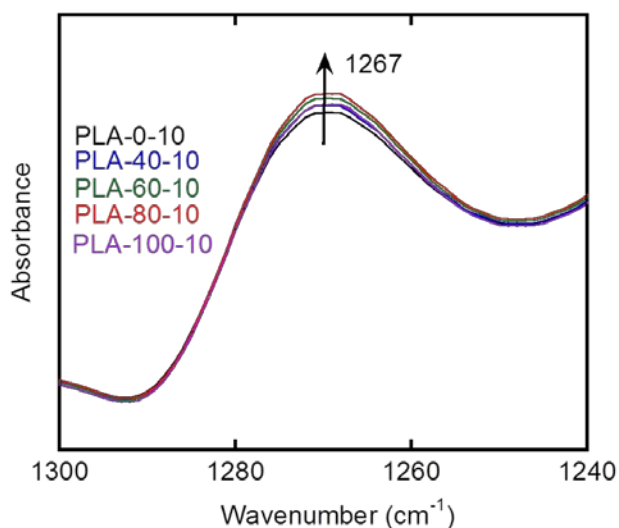


**Figure 9.** FT-IR spectra for the samples cooled at various temperatures.

Since the packing density of chains plays the decisive role in the deformation mechanism, the post-processing annealing operation must provide the same impact on the tensile behavior for PLA. Figure 10 shows the stress-strain curves for the samples with and without the annealing operation at 60 °C for 10 min, using PLA-40-10. Although the sample without the annealing shows brittle fracture, the annealing procedure changes the fracture mechanism from brittle to ductile. Moreover, the slight increase in  $T_g$  is also detected by the dynamic mechanical analysis after the annealing, as shown in Figure 11. The sample also shows a strong peak at 1267  $\text{cm}^{-1}$  in the FT-IR spectra. The results support our finding that a high population of *gg* conformers caused by the conformation change is responsible for the shear yielding deformation despite the closed packing of polymer chains.

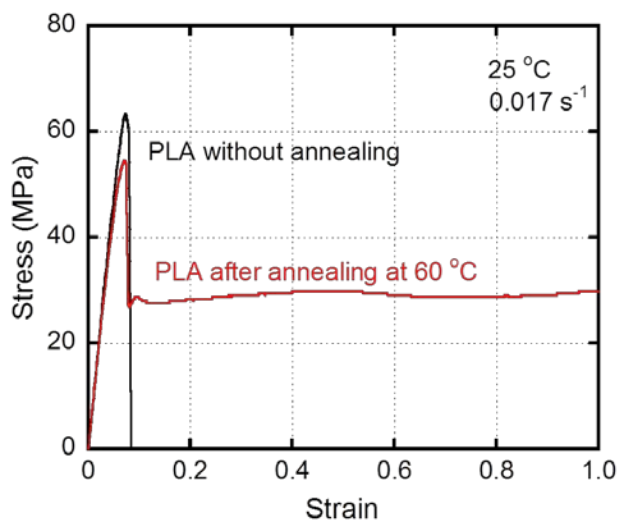


**Figure 10.** Stress-strain curves for the samples with and without post-processing annealing operation at 60 °C for 10 min.

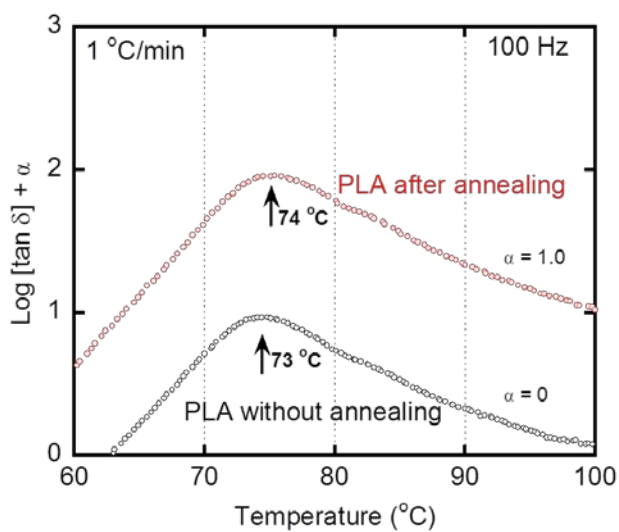


**Figure 11.** Temperature dependence of loss tangent  $\tan \delta$  at 100 Hz for the samples with and without post-processing annealing at 60 °C for 10 min. (black open circles) PLA without post-annealing operation at 60 °C for 10 min, and (red open circles) PLA with post-annealing operation at 60 °C for 10 min.

The anomalous effect of the post-processing annealing should be noted for industrial applications. Furthermore, the effect of cooling temperature on mechanical toughness should be considered seriously for the industrial applications, because it can be controlled during actual processing operations.

## Conclusions

The tensile behaviors of amorphous PLA films obtained by compression-molding were investigated. It is found that the samples cooled at temperatures slightly higher than  $T_g$ , e.g., 60 and 80 °C, show ductile behavior at room temperature, with a low brittle-ductile transition temperature. In contrast, the other cooling temperatures, e.g., 0, 40, and 100 °C, provide brittle samples, which is a typical mechanical behavior of PLA. Moreover, the mechanical toughness of the samples cooled at 56 °C increases with increasing cooling time. The ductile deformation occurs even for the quenched samples after annealing operation at 60 °C for 10 min.

Because of the thermal history near  $T_g$ , the ductile samples have the high level of chain packing, which is confirmed by high  $T_g$ . Although the closed chain packing is believed to be responsible for brittle fracture for most plastics owing to the enhancement of critical onset stress for shear yielding, the increase in the specific conformer, i.e., *gg*, leads to the conformation change under the low stress level. Consequently, shear yielding, i.e., ductile deformation, occurs as a dominant deformation mechanism for PLA. In other words, the mechanical toughness of PLA can be improved greatly by the appropriate processing operation.

## References

1. Auras, R.; Lim, L. T.; Selke, S. E. M.; Tsuji, H. *Poly(lactic acid): synthesis, structures, properties, processing, and applications*. Wiley: New Jersey, 2010.
2. Jimenez, A.; Peltzer, M.; Ruseckaite, R. *Poly(lactic Acid) Science and Technology: Processing, Properties, Additives, and Applications*. Royal Society of Chemistry: Oxfordshire, 2014.
3. Lim, L. T.; Auras, R.; Rubino, M.; *Prog. Polym. Sci.* **2008**, 33, 820-852.
4. Rasal, R. M.; Janorkar, A. V.; Hirt, D. E. *Prog. Polym. Sci.* **2010**, 35, 338-356.
5. Saeidlou, S.; Huneault, M. A.; Li, H. B.; Park, C. B. *Prog. Polym. Sci.* **2012**, 37, 1657-1677.
6. Grijpma, D. W.; Penning, J. P.; Pennings, A. J. *Colloid Polym. Sci.* **1994**, 272, 1068-1081.
7. Auras, R.; Harte, B.; Selke, S. *Macromol. Biosc.* **2004**, 4, 835-864.
8. Kowalczyk, M.; Piorkowska, E. *J. Appl. Polym. Sci.* **2012**, 124, 4579-4589.
9. Zhang, C.; Wang, W.; Huang, Y.; Pan, Y.; Jiang, L.; Dan, Y.; Luo, Y.; Peng, Z. *Mater. Des.* **2013**, 45, 198-205.
10. Zhao, Q.; Ding, Y.; Yang, B.; Ning, N.; Fu, Q. *Polym. Test.* **2013**, 32, 299-305.
11. Kinloch, A. J.; Young, R. J. *Fracture behavior of polymers*, Applied Science Publishers: London and New York, 1983.
12. Kausch, H. H. *Polymer Fracture*, Springer-Verlag: Berlin, 1987.
13. Ward, I. M.; Hadley, D. W. *An introduction to the mechanical properties of solid polymers*, Wiley: UK, 1993.

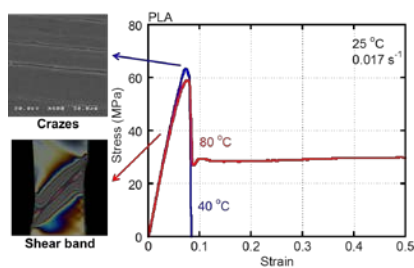
14. Argon, A. S. *The physics of deformation and fracture of polymers*, Cambridge University Press: New York, 2013.
15. Kambour, R. P. *J. Polym. Sci.* **1973**, 7, 1-154.
16. Narisawa, I.; Kuriyama, T.; Ojima, K. *Makromol. Chem., Macromol. Symp.* **1991**, 41, 87-107.
17. Meijer, H. E. H.; Govaert, L. E. *Prog. Polym. Sci.* **2005**, 30, 915-938.
18. Lee, H. N.; Ediger, M. D. *Macromolecules* **2010**, 43, 5863-5873.
19. Deblieck, R. A. C.; Van Beek, D. J. M.; Remerie, K.; Ward, I. M. *Polymer* **2011**, 52, 2979-2990.
20. Vincent, P. I. *Polymer* **1960**, 1, 425-444.
21. Stearne, J. M.; Ward, I. M. *J. Mater. Sci.* **1969**, 4, 1088-1096.
22. Van Melick, H. G. H.; Govaert, L. E.; Meijer, H. E. H. *Polymer* **2003**, 44, 3579-3591.
23. Cheng, S.; Johnson, L.; Wang, S. Q. *Polymer* **2013**, 54, 3363-3369.
24. Pan, P.; Zhu, B.; Inoue, Y. *Macromolecules* **2007**, 40, 9664-9671.
25. Vleeshouwers, S.; Nies, E. *Thermochim Acta.* **1994**, 238, 371-395.
26. Hadac, J.; Slobodia, P.; Rina, P.; Saha, P.; Rychwalski, R. W.; Emri, I.; Kubat, J. *J. Non-Cryst. Solids* **2007**, 353, 2681-2691.
27. Allen, G.; Morley, D. C. W.; Williams, T. *J. Mater. Sci.* **1973**, 8, 1449-1452..
28. Robertson, R. E. *Appl. Polym. Symp.* **1968**, 7, 201.
29. Kambour, R. P.; Robertson, R. E. In: *Polymer science*, Jenkins, A. D. Ed., Northholland: London, **1972**; p 688-822.

30. Argon, A. S.; Bessonov, M. I. *Polym Eng Sci* **1977**, 17, 174-182.
31. Pan, P.; Zhu, B.; Dong, T.; Yazawa, K.; Shimizu, T.; Tansho, M.; Inoue, Y. *J. Chem. Phys.*, **2008**, 129, 184902-184911.
32. Kister, G.; Cassanas, G.; Vert, M. *Polymer* **1998**, 39, 267-273.

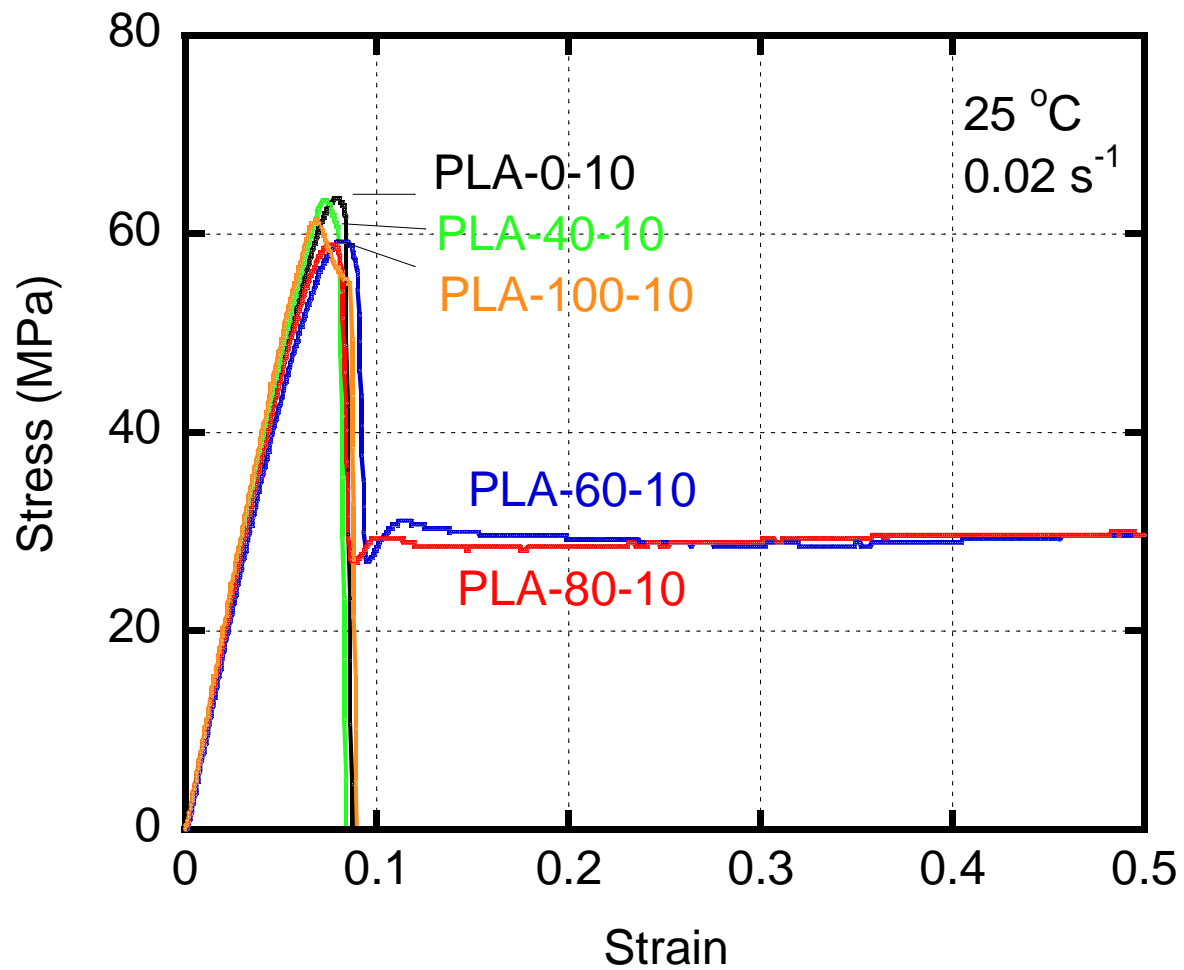
For Table of Content use only

Chain packing and its anomalous effect on mechanical toughness for poly(lactic acid)

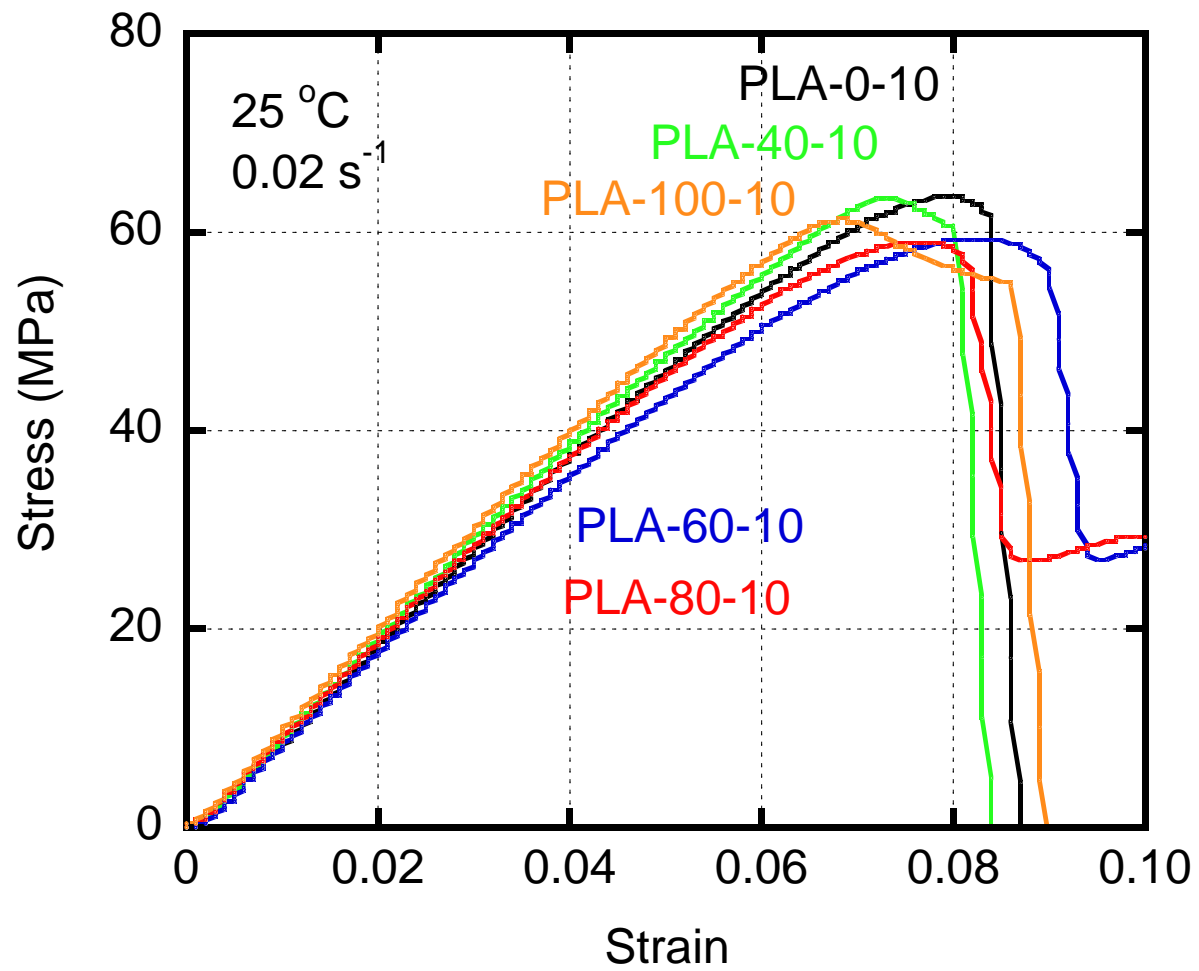
Tong Huang, Motohiro Miura, Shogo Nobukawa, Masayuki Yamaguchi\*





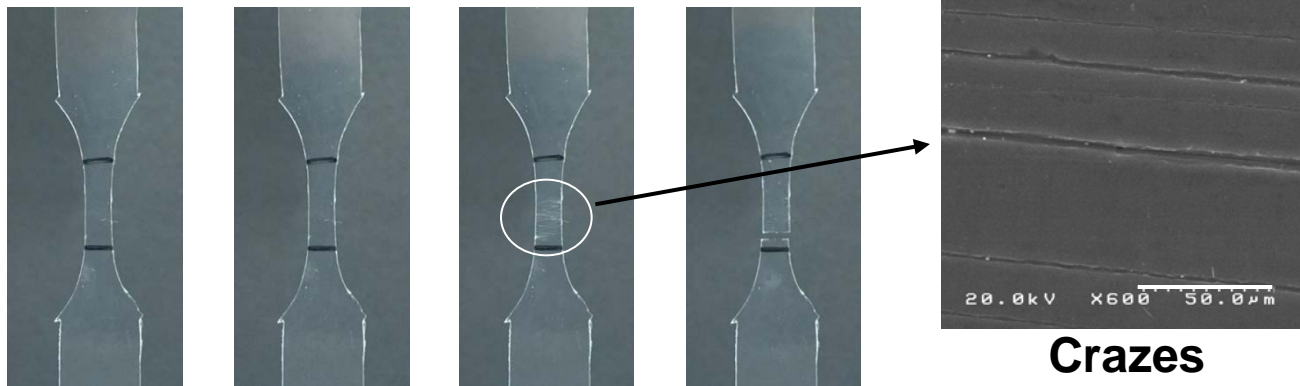


Huang et al., Fig. 1



**PLA-40-10**

(a)



**PLA-80-10**

(b)

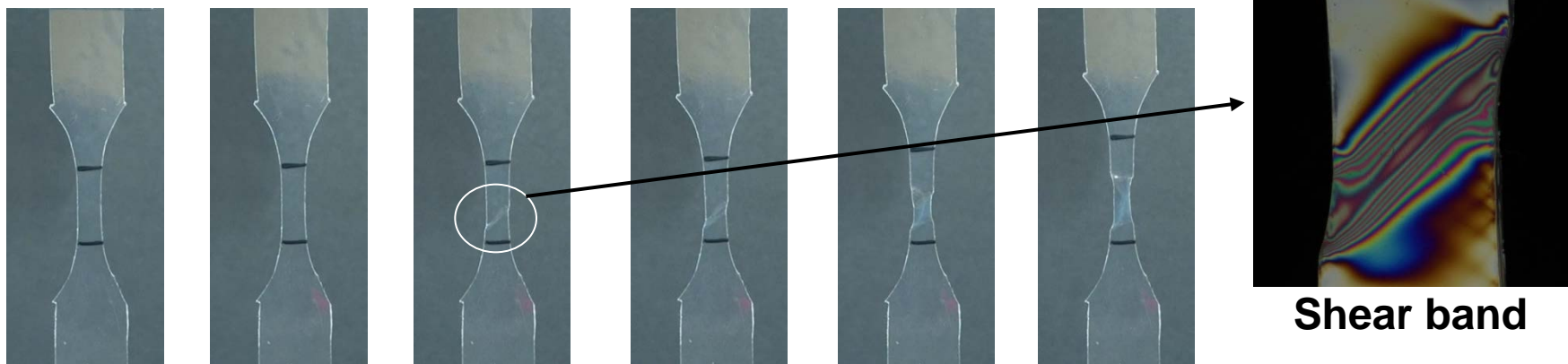
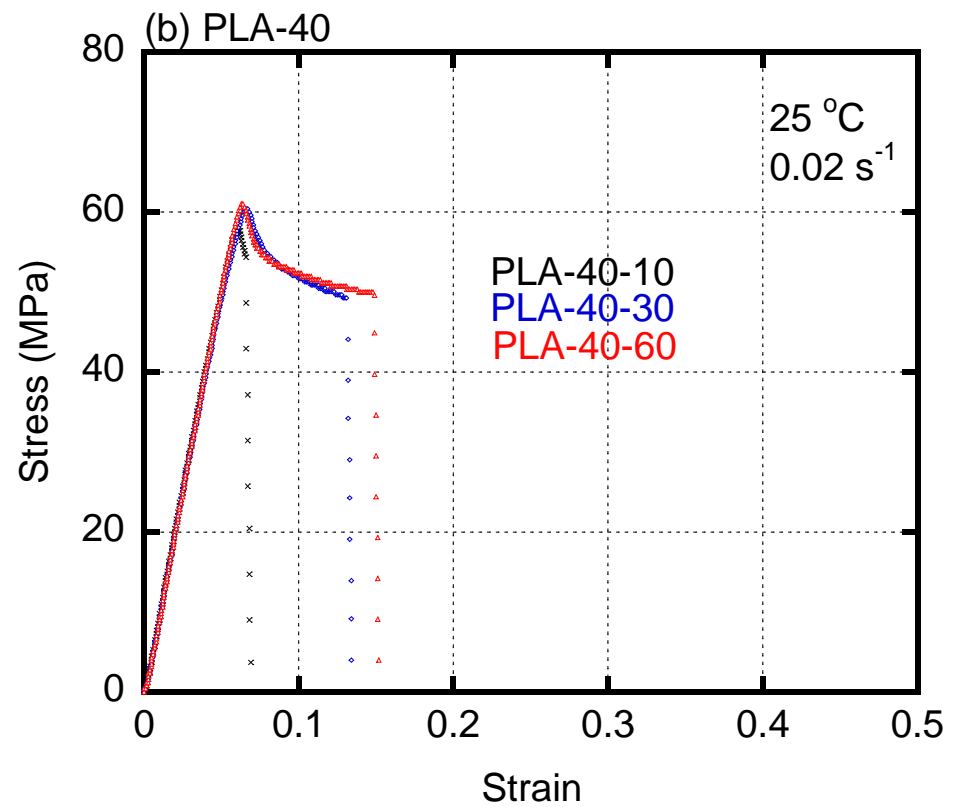
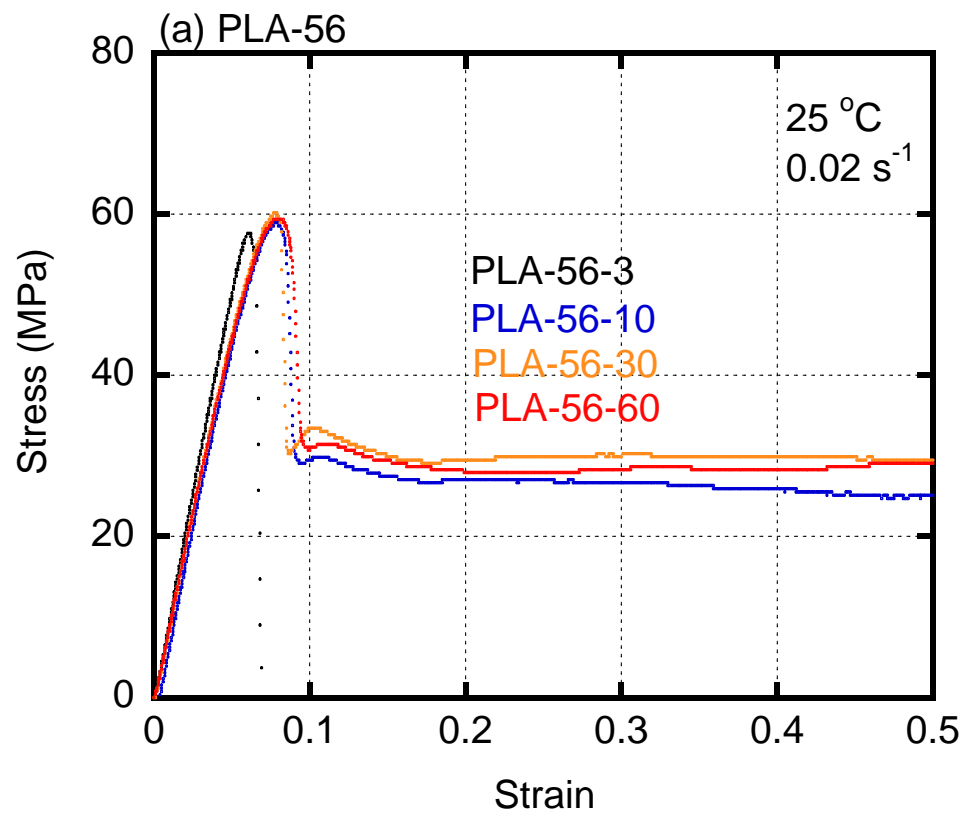
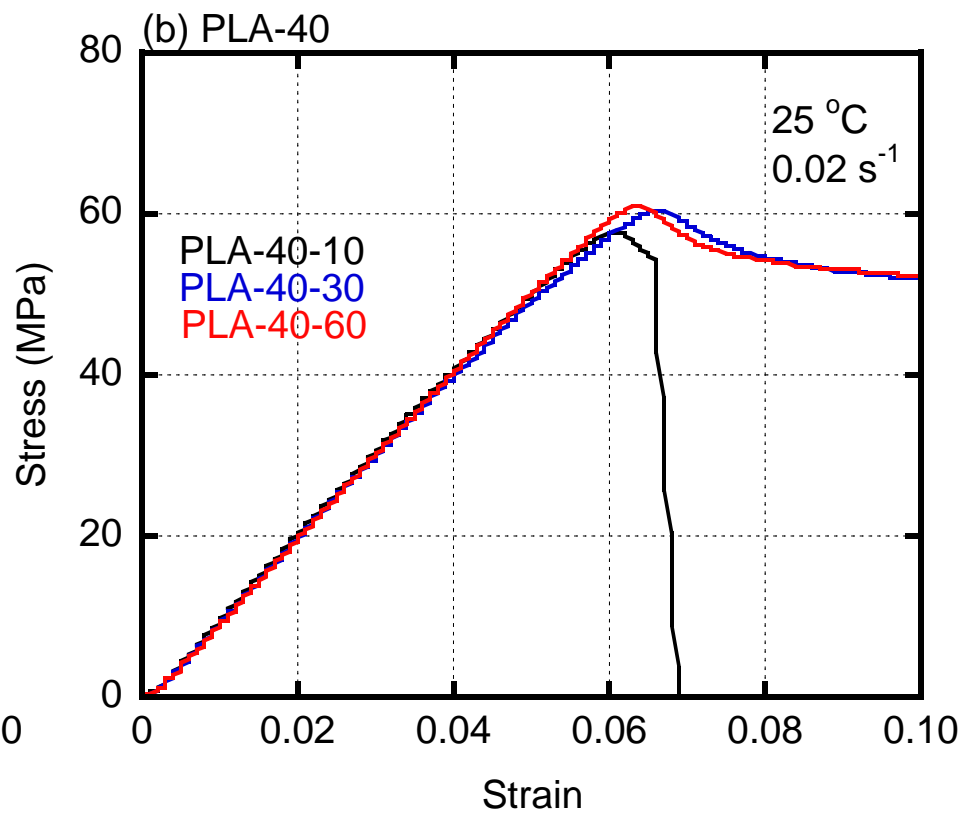
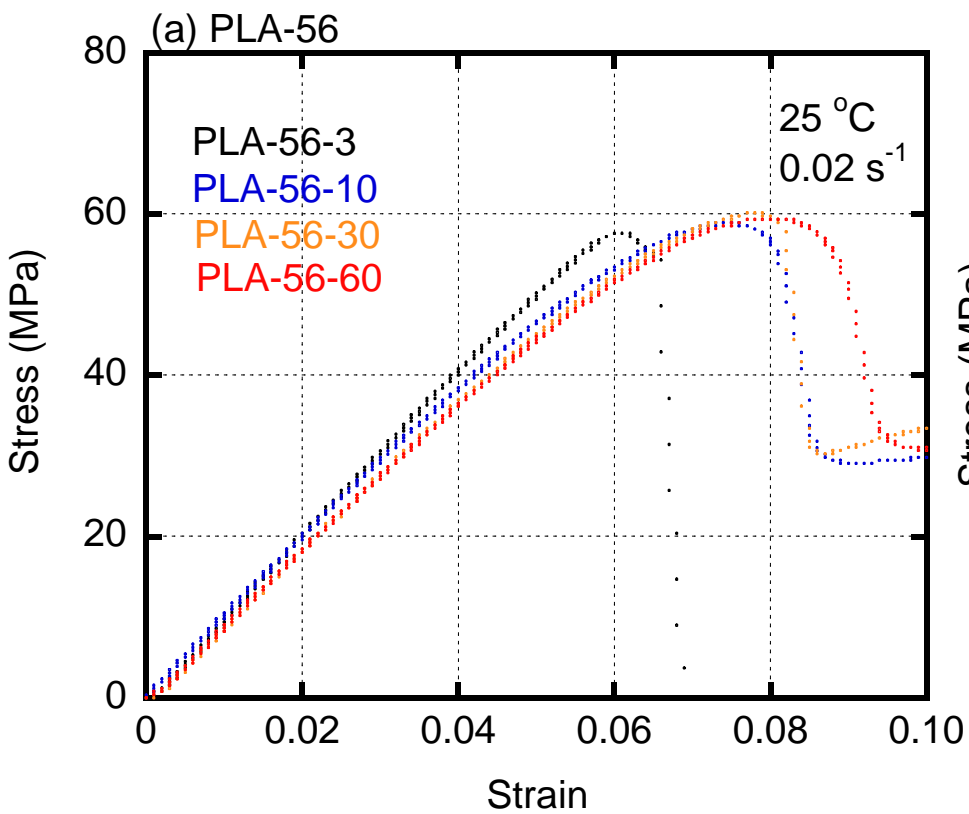


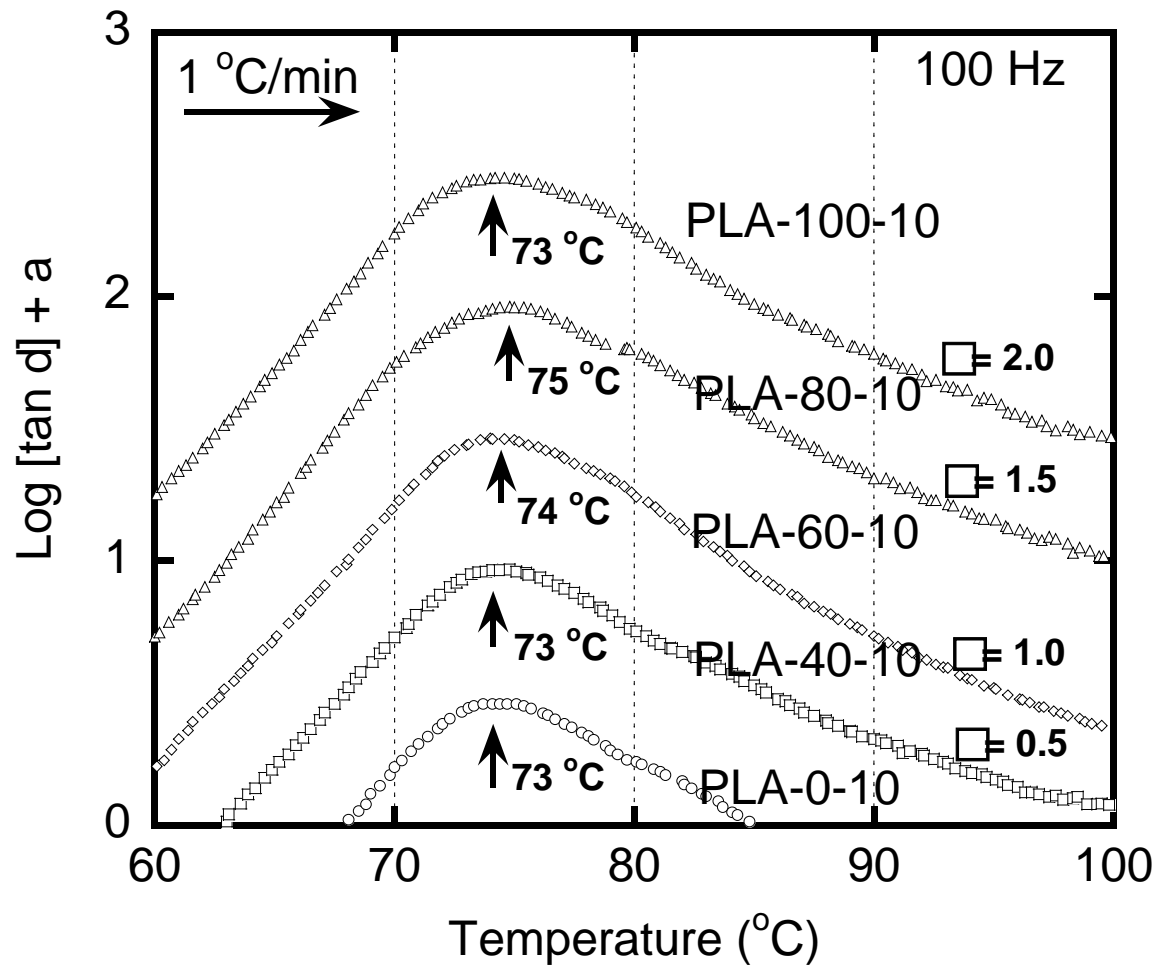
Table 1. Mechanical properties of PLA samples cooled at various temperatures

<b>Samples</b>	<b>Strain at break</b>	<b>Tensile Yield Stress (MPa)</b>	<b>Young's Modulus (MPa)</b>
PLA-0-10	$0.079 \pm 0.002$	$63.6 \pm 1.3$	805
PLA-40-10	$0.077 \pm 0.001$	$61.1 \pm 1.6$	794
PLA-60-10	> 3	$60.2 \pm 2.2$	792
PLA-80-10	> 3	$58.1 \pm 1.4$	796
PLA-100-10	$0.078 \pm 0.004$	$61.4 \pm 1.7$	787

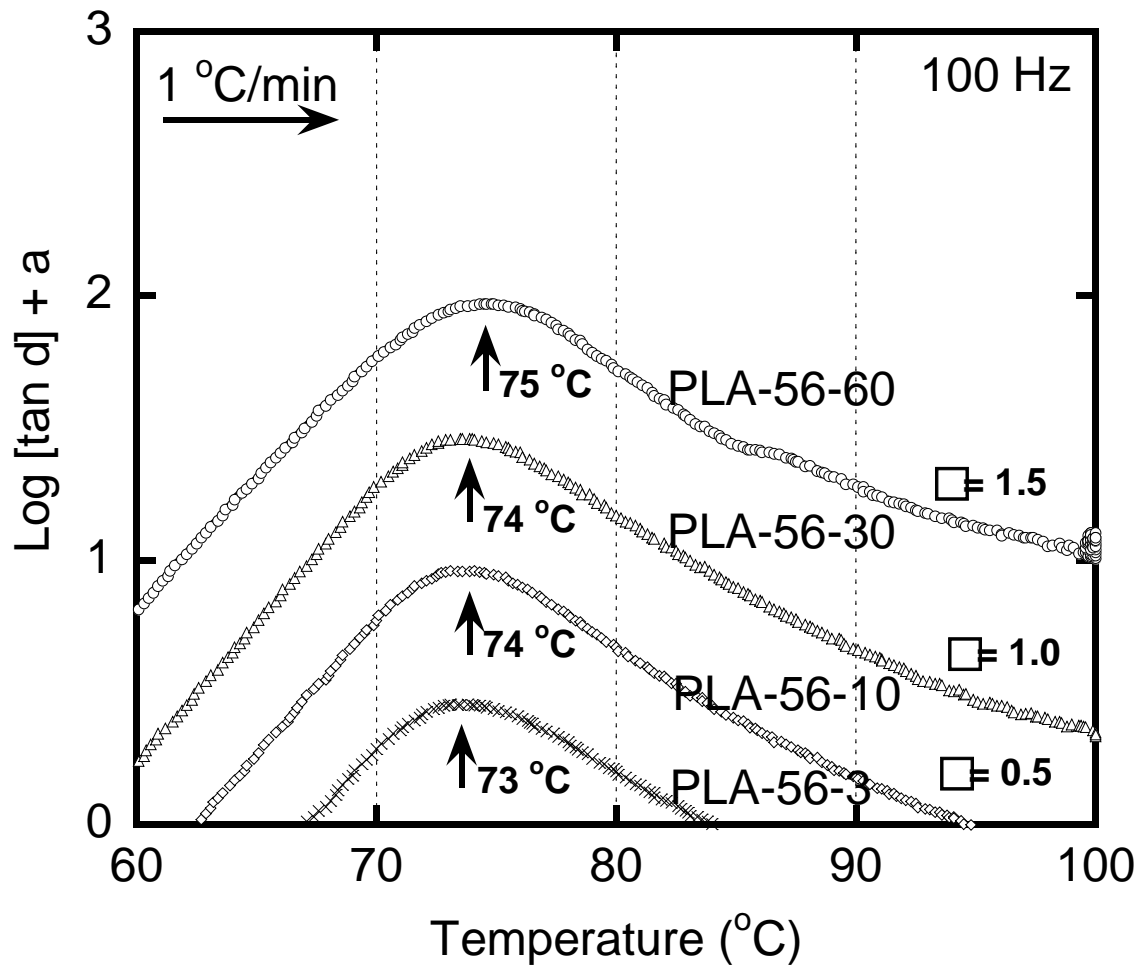


Huang et al., Fig. 3





Huang et al., Fig. 4



Huang et al., Fig. 5

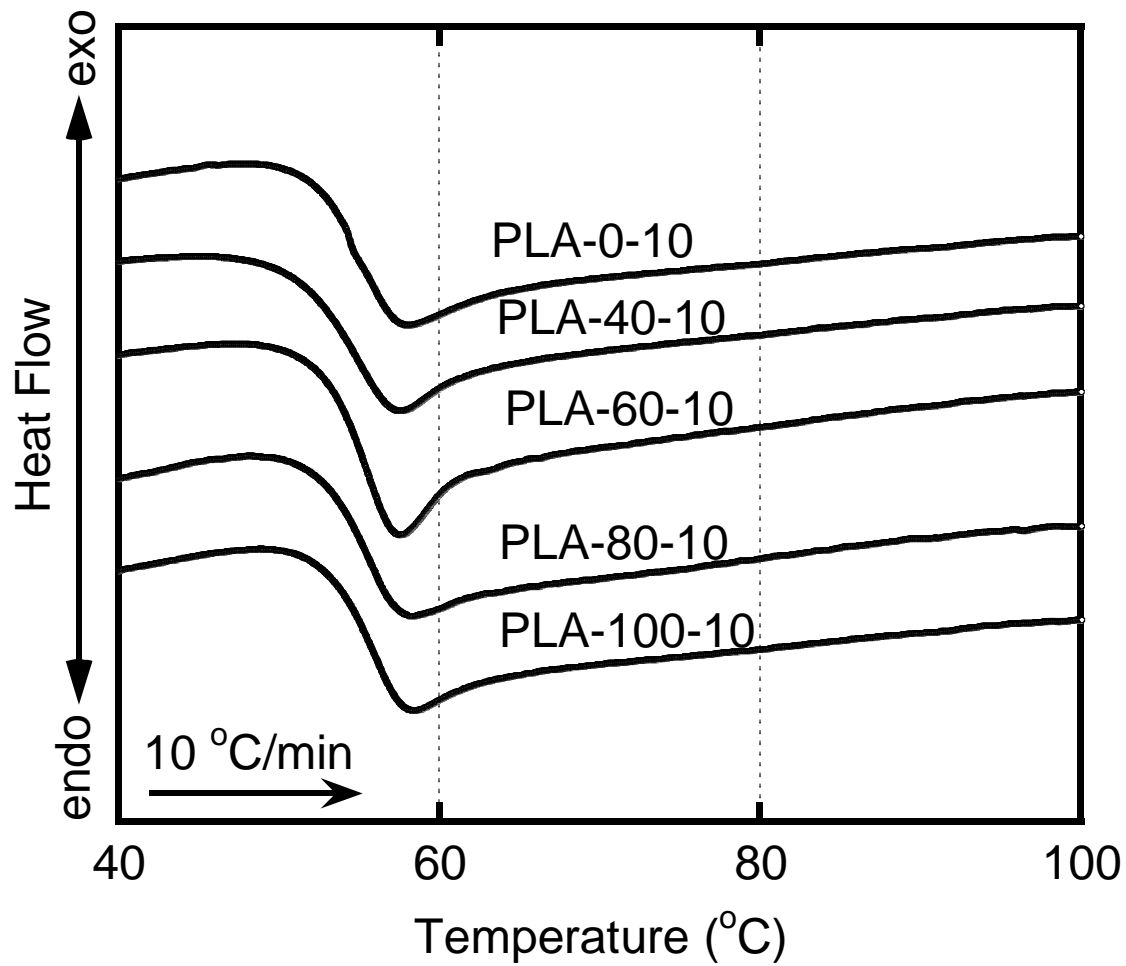


Table 2. Glass transition temperature  $T_g$  of samples cooled at various temperatures

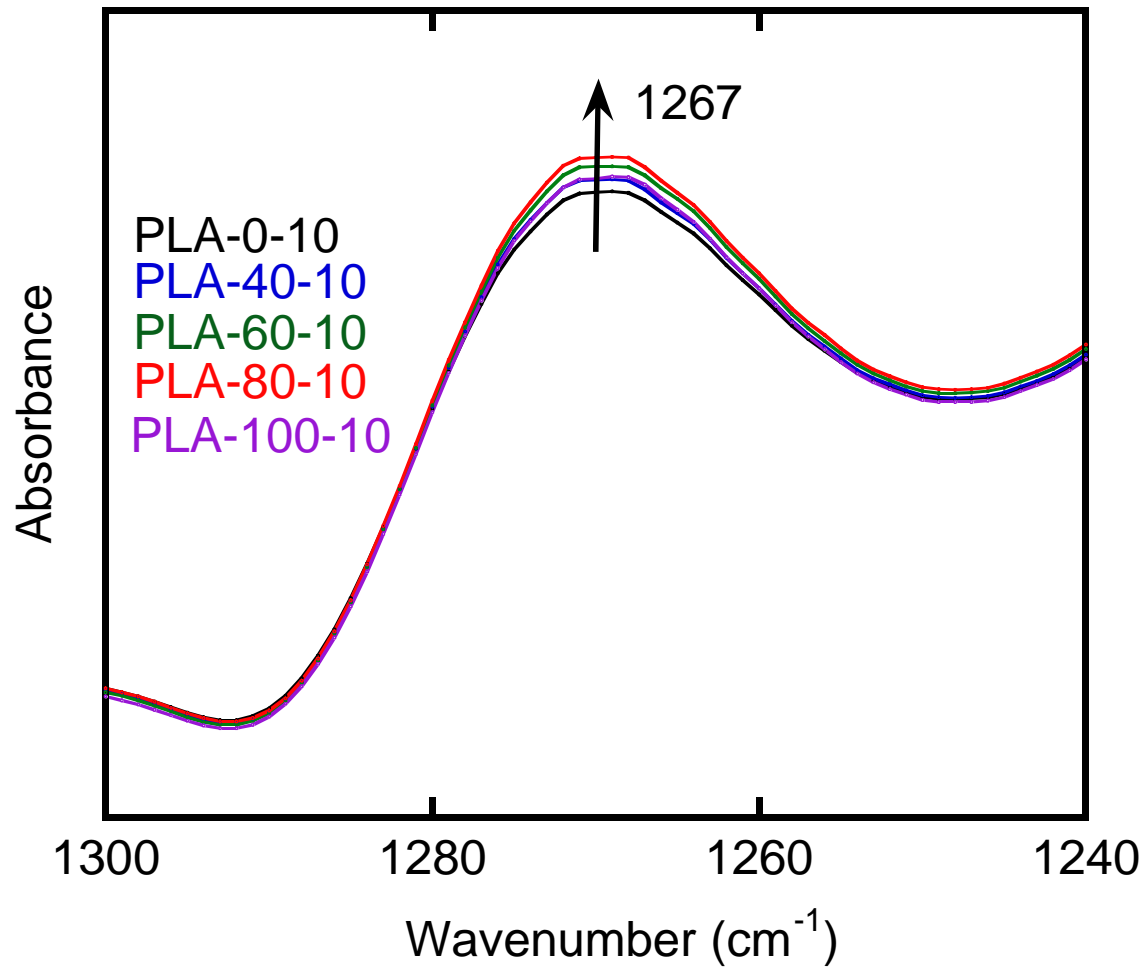
<b>Samples</b>	<b><math>T_g^a</math>(°C)</b>	<b><math>T_g^b</math>(°C)</b>
PLA-0-10	73	53
PLA-40-10	73	53
PLA-60-10	74	54
PLA-80-10	75	55
PLA-100-10	73	53

<sup>a</sup>  $T_g$  is determined by DMA.

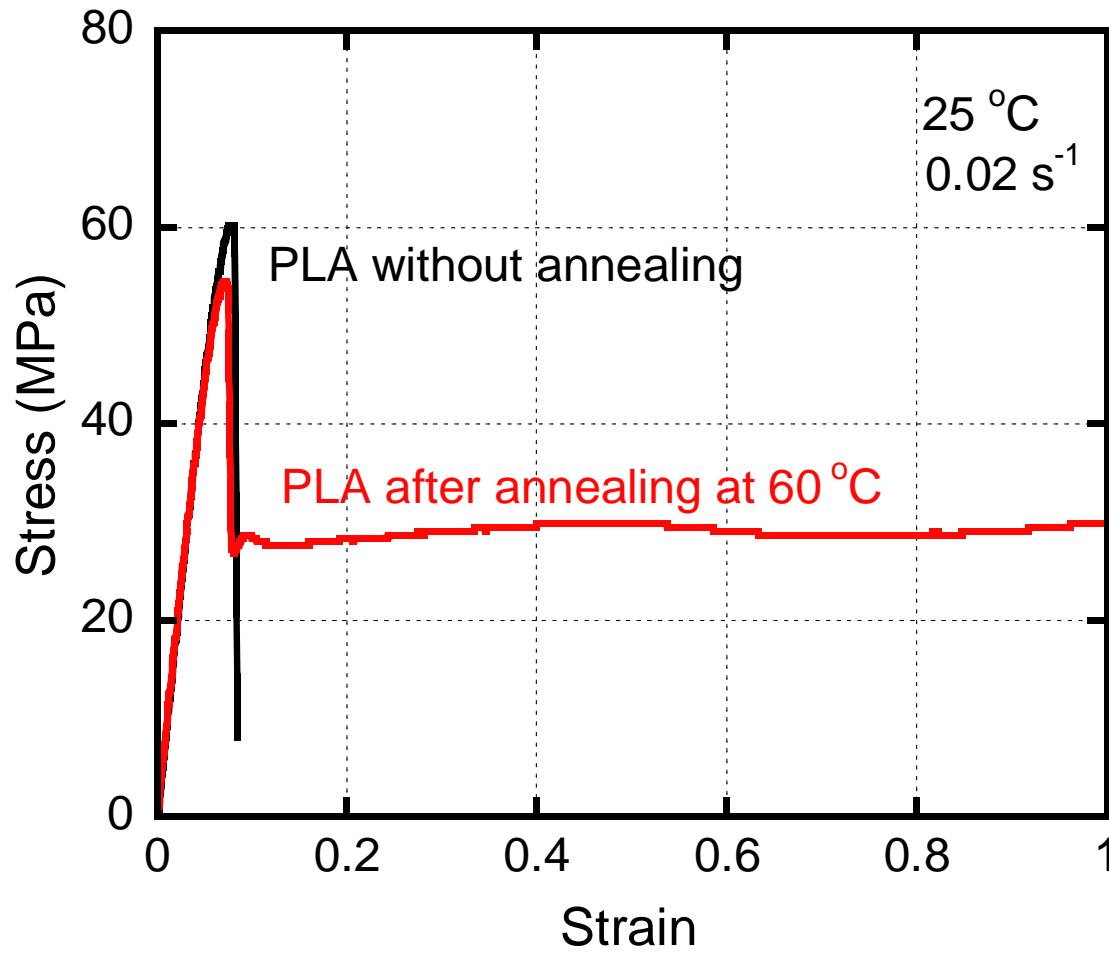
<sup>b</sup>  $T_g$  is determined by DSC.



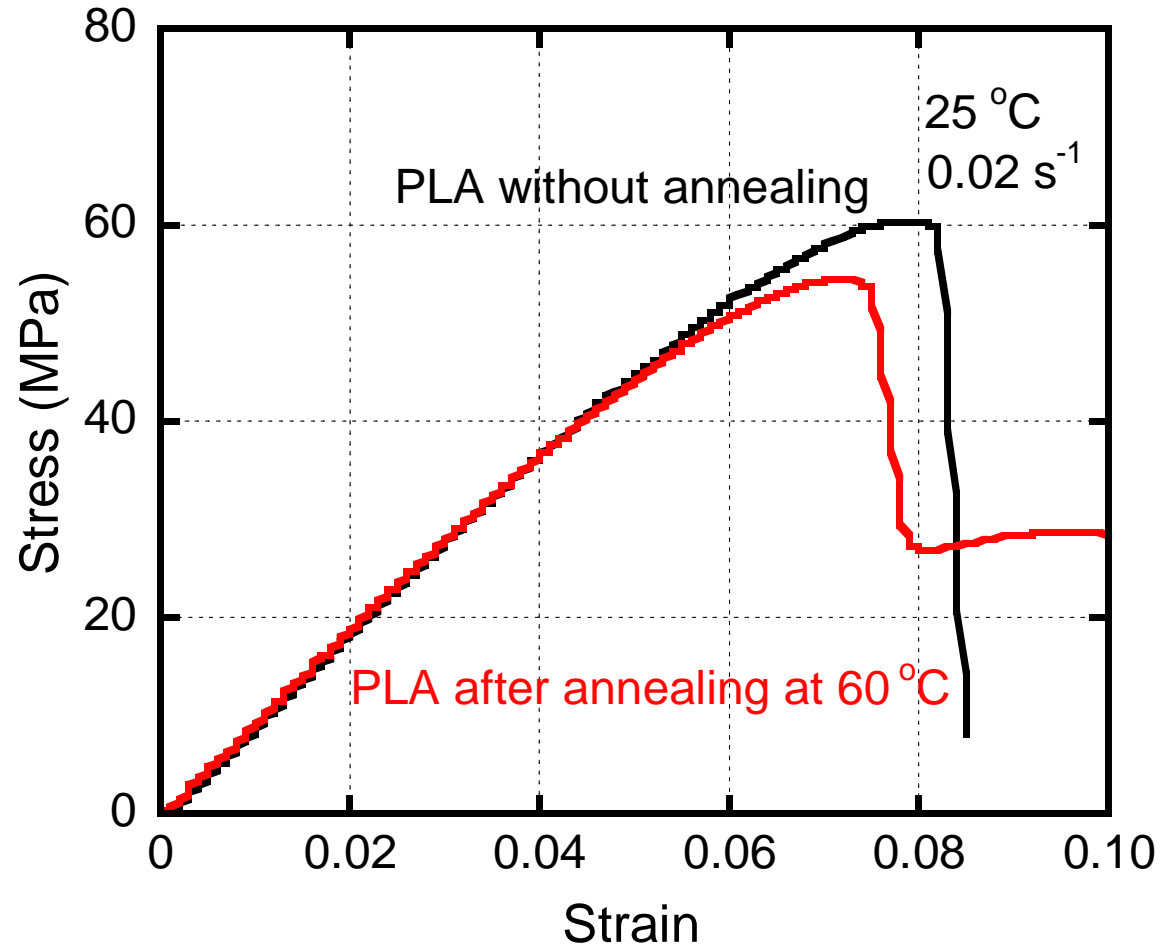
Huang et al., Fig. 6

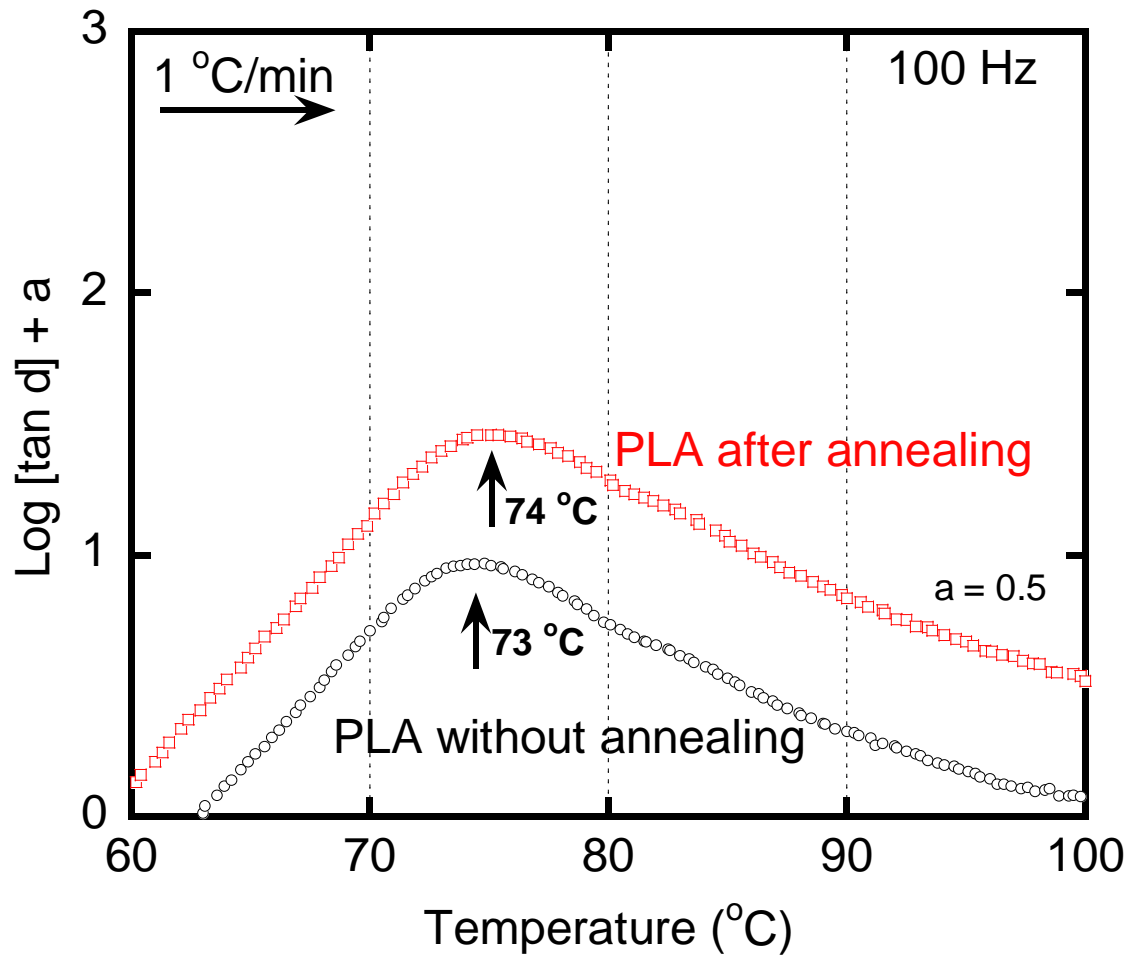


Huang et al., Fig. 7



Huang et al., Fig. 8





Huang et al., Fig. 9

